Enantioselective synthesis of polysubstituted prolines by Binap-silver-catalyzed 1,3-dipolar cycloadditions

Carmen Nájera [a,*], M. de Gracia Retamosa [a], José M. Sansano [a,*], Abel de Cózar [b], Fernando P. Cossío [c,†]

[a] *Departamento de Química Orgánica e Instituto de Síntesis Orgánica (ISO), Facultad de Ciencias, Universidad de Alicante, Apartado 99, 03080 Alicante, Spain*
[b] *Area de Química Orgánica, Universidad de Castilla-La Mancha, E-13071 Ciudad Real, Spain*
[c] *Departamento de Química Orgánica I, Facultad de Química, Universidad del País Vasco—Euskal Herriko Unibertsitatea, P. K. 1072, E-20018 San Sebastián-Donostia, Spain*

ABSTRACT

The enantioselective 1,3-dipolar cycloaddition reaction of stabilized azomethine ylides, generated from iminoesters, with maleimides was efficiently achieved by intermediacy of an equimolar mixture of chiral (*R*)- or (*S*)-Binap and AgClO$_4$. The high stability of the titled catalytic metal-complex to light exposure and its insolubility in toluene made possible its recovery and reutilization in other new process. In order to get a better understanding of the behavior of these chiral catalysts, we have carried out DFT1 calculations demonstrating the experimentally observed high enantio- and *endo*-selectivity through a very asynchronous transition state.

© 2009 Elsevier Ltd. All rights reserved.

1. Introduction

Proline is singular among the genetically encoded α-amino acids (α-AA) due to the rigidity conferred by its pyrrolidine ring, which leads to a steric hindrance that is useful in the design of biologically active peptides,[1] including the proline rich amphiphatic cell-penetrating peptides.[2] Substitution on the pyrrolidine heterocycle opens new perspectives on these areas, especially in structure–activity relationships studies of the newly generated peptides.[1] Restriction of the conformational space concerns not only proline or its derivative, but also the preceding residue. The substituent attached at the 2-position of the heterocycle (α-methylation) is widely used to stabilize the helical conformation of peptides, as well as some type I β-*trans* arrangements. However, substitution at the 3-position has not been much studied, and the results are not so predictable. Substituted prolines at the 4-position can be considered as a constrained analogues of homocysteine glutamate, homoarginine, and homoserine depending on the nature of the functional group used as a substituent. These 4-substituted surrogates, together with prolines incorporating a substituent at the 5-position, are used to stabilize type VI β-turns conformations and favor the preference of the C^V-*exo*-puckering in the peptide.[1]

The proline-derived structures themselves have been employed as organocatalyst[3] in many useful transformations and also as potent drugs. For example, antiviral agents **1** are active products against the hepatitis C virus,[4] kainoids **2** possess neuro-excitatory activity and can be also used as insecticides,[5] and (−)-dysibetaine **3** is a known neuroexcitotoxin.[6] Hydroxyprolines **4** and **5** are crucial in collagen catabolism, and for the stabilization of protocollagens and glycoproteins in plants and animals,[7] respectively (Fig. 1).
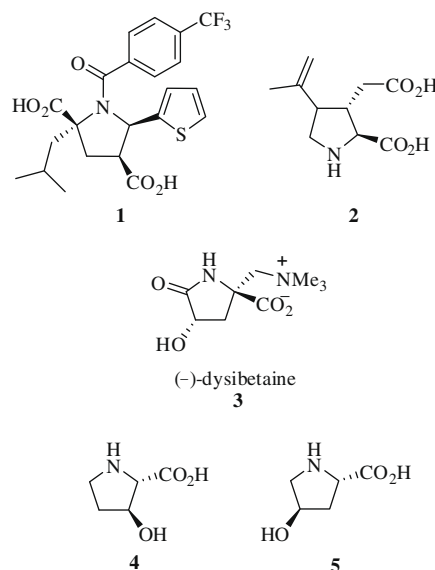

Figure 1. Some biologically active proline derivatives.

* Corresponding authors. Fax: +34 96 5903549 (C.N.).
E-mail addresses: cnajera@ua.es (C. Nájera), jmsansano@ua.es (J.M. Sansano).
† For correspondence on computational studies:fp.cossio@ehu.es.

The synthesis of enantioenriched-substituted prolines[8] can be achieved by several routes, as for example, starting from prolines or proline derivatives, and through C–N or C–C bond-forming cyclizations. These routes operate under a diastereoselective key step included in a lengthy synthetic sequence. Since 2002, several fascinating enantioselective syntheses of substituted prolines through 1,3-dipolar cycloaddition[9] (1,3-DC) of azomethine ylides and electron poor alkenes have been developed by several groups.[10] The simultaneous formation of the three or four new stereocenters of the resulting pyrrolidine can be achieved using chiral complexes of silver,[11] copper,[12] zinc,[13] nickel,[14] calcium,[15] or chiral organocatalysts,[16] the metal-catalyzed reaction being the most efficient and reliable route. Particularly, the most elevated *endo/exo* diastereoselectivities and enantioselectivities were obtained with mono- or bidentate chiral ligands Ag^I or Cu^I complexes.

The combination of (*S*)-Binap–AgOAc showed low ee in 1,3-DC when dipoles derived from iminoesters and dimethyl maleate (up to 13% ee),[11a] or phenyl vinyl sulfone (up to 26% ee),[12e,i] were used as dipolarophiles. In our group, we have used the Binap ligand[17] and AgClO$_4$ to generate active catalysts in the 1,3-DC using *N*-methylmaleimide (NMM) and iminoesters.[11h] In this work, we will describe the scope of this reaction, the study of another diphosphines as well as the origin of the elevated enantioselectivity and *endo*-diastereoselectivity.

2. Results and discussion

2.1. Optimization of the reaction conditions

The selected model reaction between methyl benzylideneiminoglycinate **6aa** and NMM **7** was carried out in toluene at room temperature using 5 mol % of (*S*)-Binap **8** and 5 mol % of Ag^I salt as catalyst precursor (Scheme 1, Table 1).

The reaction run with an equimolar amount of both Binap **8** and silver(I) salts such as AgBF$_4$, AgNO$_3$, and Ag$_2$O (5 mol %) gave poor results in terms of enantioselectivity and conversion (Table 1, entries 1–3). When AgOAc was used, excellent results of the compound **6aa** were obtained (Table 1, entry 4), but the crude reaction product was not as clean as in the case of AgClO$_4$ does. AgOTf and AgF were also tested giving irreproducible results in both cases (Table 1, entries 5 and 6). However, reproducible results
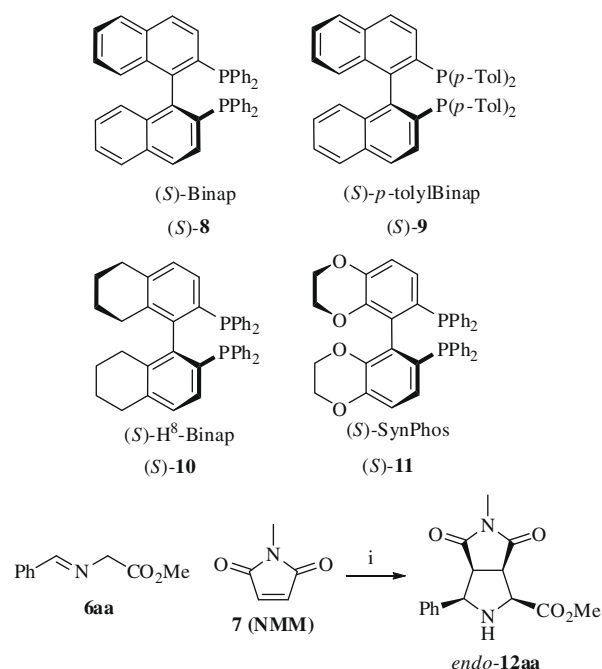
Scheme 1. Reagents and conditions: (i) (*S*)-Diphosphine (5 mol %), Ag^I salt (5 mol %), Et$_3$N (5 mol %), toluene, rt, 16 h.

of a very clear crude **12aa** product with excellent enantioselectivities (>99% ee), high *endo*-diastereoselectivity (>98/2), and 90% yield were achieved with AgClO$_4$ (Table 1, entry 7). Just 3 mol % of the catalytic complex also gave good enantioselectivities, but the reaction time was too long (1.5 d, Table 1, entry 8). This AgClO$_4$ was used rather than the corresponding monohydrate because the last compound was more difficult to weight (Table 1, entry 9). Next, different ratios of Binap/AgClO$_4$ were tested. Thus, when a 2:1 mixture of Binap/AgClO$_4$ was added (Table 1, entry 10), the percentage of the *exo*-cycloadduct was increased. When a 1:2 mixture was prepared in situ, the product **12aa** was obtained with a very low enantioselectivity (Table 1, entry 11). In summary, the equimolar Binap/AgClO$_4$ was definitively the most efficient complex for this process (compare entries 7, 10, and 11).

Table 1
Optimization of the reaction of iminoesters **6a** with NMM

Entry	Iminoester **6**	Ligand	Ag^I salt	Product **12**[a]			
				No.	Yield (%)[b]	*endo/exo*[c]	ee (%)[d]
1	**6aa**	**8**	AgBF$_4$	**12aa**	77	89:11	72
2	**6aa**	**8**	AgNO$_3$	**12aa**	65	85:11	67
3	**6aa**	**8**	Ag$_2$O	**12aa**	65	90:10	18
4	**6aa**	**8**	AgOAc	**12aa**	89	>98:2	99
5	**6aa**	**8**	AgOTf	**12aa**	88	90:10	99
6	**6aa**	**8**	AgF	**12aa**	81	90:10	98
7	**6aa**	**8**	AgClO$_4$	**12aa**	90	>98:2	>99
8	**6aa**	**8**	AgClO$_4$[e]	**12aa**	90	>98:2	>99
9	**6aa**	**8**	AgClO$_4$·H$_2$O	**12aa**	89	>98:2	99
10	**6aa**	**8**	AgClO$_4$[f]	**12aa**	89	90:10	98
11	**6aa**	**8**	AgClO$_4$[g]	**12aa**	91	90:10	<50
12	**6aa**	**9**	AgClO$_4$	**12aa**	91	>98:2	>99
13	**6aa**	**10**	AgClO$_4$	**12aa**	90	>98:2	>99
14	**6aa**	**11**	AgClO$_4$	**12aa**	90	>98:2	98

[a] The conversions were higher than 95% (determined by ^{1}H NMR spectroscopy).
[b] Isolated yield after recrystallization.
[c] Determined by ^{1}H NMR spectroscopy of the crude product.
[d] Determined by chiral HPLC (Daicel Chiralpak AS) of the recrystallized product.
[e] Reaction performed with a 3 mol % of the catalyst taking more than 1.5 d to complete.
[f] Reaction performed with 2 equiv of **8** and 1 equiv of AgClO$_4$.
[g] Reaction performed with 1 equiv of **8** and 2 equiv of AgClO$_4$.

The effect of solvent was also important because almost racemic mixtures were obtained with diethyl ether, whilst dichloromethane and THF gave moderate enantioselectivities (<60% ee) of product **12aa**.

Three additional diphosphines (**9**–**11**) were evaluated in this particular model reaction (Scheme 1). It is very well known that improvements of the enantioselectivity promoted by diphosphines were associated with changes in the corresponding dihedral and bite angles of the resulting chiral metal complex.[18] Thus, equimolar mixtures of silver perchlorate and ligands **9**, **10**, and **11** (5 mol% each) afforded cycloadduct *endo*-**12aa** with very high conversions and excellent enatioselectivities (>99% ee) except in the example of the reaction product generated by the intermediacy of the chiral ligand **11**, which was isolated with 98% ee (Table 1, entries 12–14).

According to these data, the Ag^I complex formed with (*R*)- and (*S*)-Binap **8** exhibited almost identical enantiodiscrimination other than the complexes generated from more expensive chiral ligands **9**–**11**. In addition, the resulting equimolar Binap–AgClO$_4$ can be recovered more easily than the analogous complexes generated from diphosphines **9**, **10**, and **11**.

The absolute configuration of the four stereocenters of known product *endo*-**14aa** (2*S*·3*R*·4*R*·5*R*) was confirmed by NOESY experiments and by comparison of the obtained data with the previous ones published in the literature.[19]

2.2. Characterization and properties of the complexes formed by (*S*)-Binap 8 and AgClO$_4$

Complexes formed from silver triflate and (*R*) or (*S*)-Binap **8** were isolated at different temperatures and further characterized by X-ray diffraction analysis by Yamamoto's group.[20] These studies revealed that mixture of structures **13**–**15** is in equilibrium and at room temperature, the 1:1 complex **14** being the most abundant system (Fig. 2).
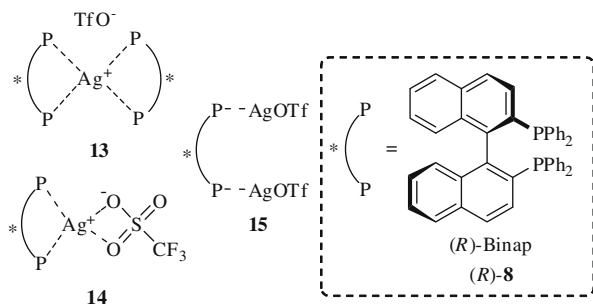

Figure 2. [(*R*)-Binap]AgOTf complexes.

In spite of equimolar [(*S*)-Binap]–AgClO$_4$ and [(*S*)-Binap]–AgOAc complexes gave identical chemical yields of product *endo*-**12aa** and very high enantioselectivity (>99 and 99% ee, respectively, Table 1, entries 4, and 7) the presumed major complex **16** was much more insoluble in toluene than the analogous formed by AgOAc. This property allowed the separation of the complex **16** from the reaction mixture by simple filtration (see Section 4). Surprisingly, complexes (*R*)- and (*S*)-**16** exhibited a high stability and any apparent decomposition occurred upon the light exposure. Both complexes **16** and **17** were prepared and isolated by reaction with 1 and 2 equiv of (*R*)- or (*S*)-Binap together to 1 equiv of AgClO$_4$, respectively. The mixture was stirred for 1 h at room temperature, and the complexes were obtained in quantitative yield. Complex (*S*)-**16** was further characterized by ESI–MS experiments showing an M$^+$+1 signal at 731 and a tiny one at 1353 (Graphic 1). In the case of complex (*S*)-**17** (Graphic 2), the same experiment revealed a peak at 1353 and a very small one at 731. However, these two
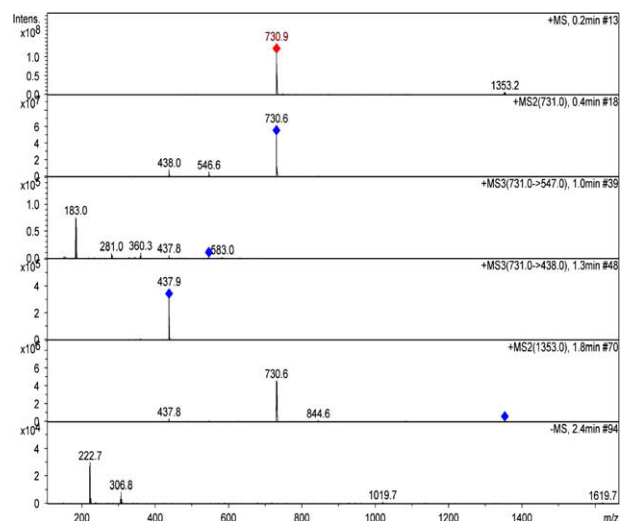
Graphic 1. ESI experiments of complex (*S*)-**16**.
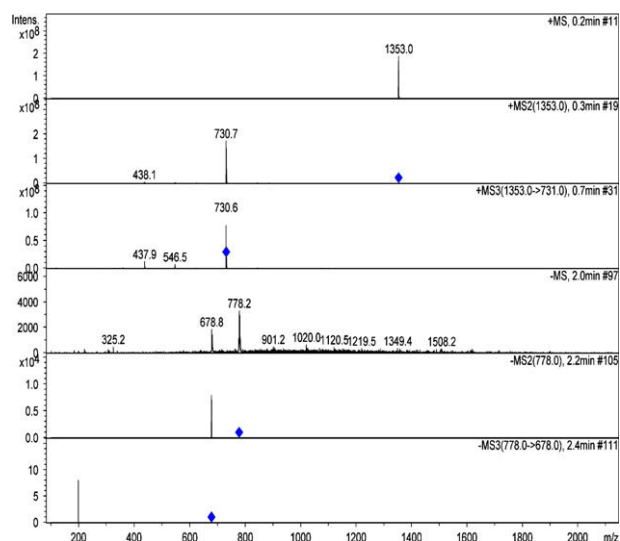
Graphic 2. ESI experiments of complex (*S*)-**17**.

in situ formed Binap complexes **16** and **17** could not be differentiated by ^{31}P NMR spectroscopy. Unfortunately, we could not obtain appropriate crystals for their comprehensive and definitive characterization by X-ray diffraction analysis (See Fig. 3).
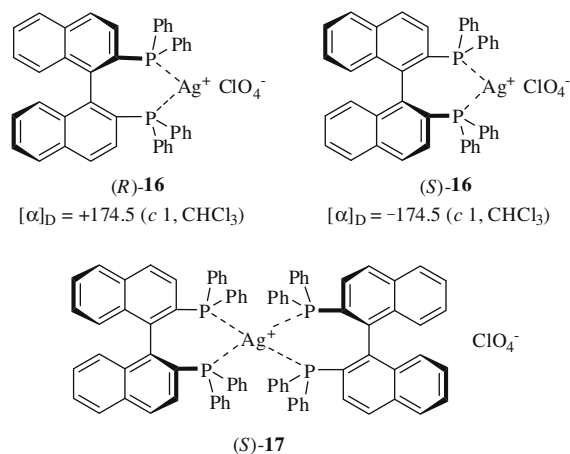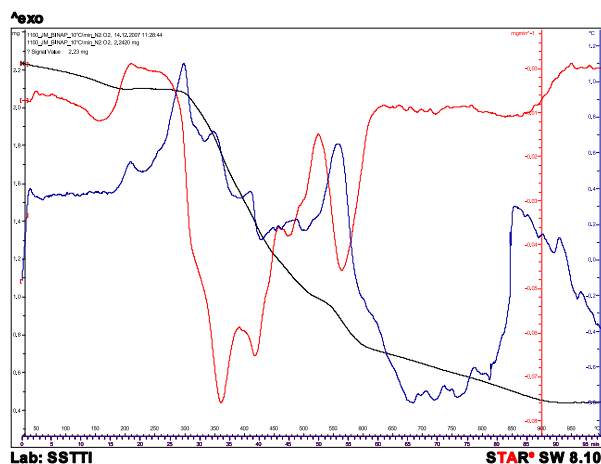

Figure 3. Structures of complexes (*R*)-**16**, (*S*)-**16**, and (*S*)-**17**.

Graphic 3. TG-DTA plot of complex (S)-**16**.

Graphic 4. NLE study of the model reaction catalyzed by the presumed major complex **16**.

Scheme 2. Reagents and conditions: (i) (S)-Binap **8** (5 mol %), AgClO$_4$ (5 mol %), base (5 mol %), toluene, rt, 16 h.

Due to the perchlorates being very hygroscopic materials and also classified as low order explosives, thermogravimetric (TG) and differential thermal analysis (DTA) of the stable species **16** were studied (Graphic 3). The integrated TG–DTA plot revealed that the loss of water of the sample occurred from 50 to 180 °C without any variation of the heat of the system. The melting point of this complex **16** is placed in Graphic 3 in the range of 209–211 °C. The three most important exothermic decomposition processes occurred approximately at 300, 550, and 860 °C.

As was described before, the easy separation of the most active major complex (S)-**16** was a very important feature to apply in a larger-scale process. So, a series of cycles were run employing the same catalytic mixture (1:1 **8**-AgClO$_4$), which was recovered and reused without any additional purification (Scheme 1 and Table 2). The reaction shown in Scheme 1 was performed on a 1 mmol scale on **6aa** with a 10 mol % of catalyst to facilitate its manipulation and successive reutilization. In the cycles 1–4, the enantioselectivity was higher than 99% ee keeping identical chemical yields (81–91%) (Table 2, entries 1–4). The fifth cycle also afforded the title product endo-**12aa** in high yield but with a slightly lower ee (98%) (Table 2, entry 5) due to the effect of the possible impurities contained in the catalyst. In all of the five cycles tested, the endo/exo diastereoselectivity was higher than 98:2 according to ^{1}H NMR experiments.

The existence of NLE was discarded when the reaction shown in Scheme 1 was performed using different enantiomeric purities of the in situ-generated major complex (S)-**16** (Graphic 4). In this case, an almost linear behavior was observed and, in consequence, it was reasonable to assume that monomeric complexes can be the catalytically active species.

2.3. Scope of the 1,3-DC catalyzed by complexes (R)- and (S)-16

The scope of the reaction employing different aryl- and ester groups at the iminoester structure with assorted dipolarophiles
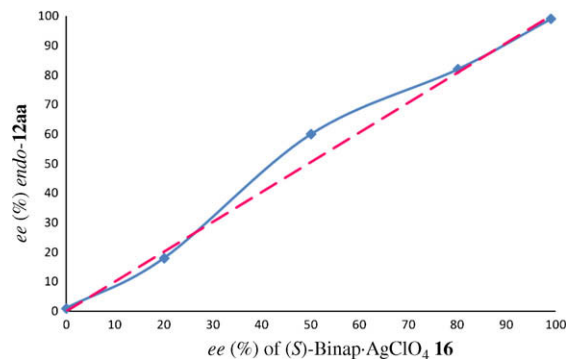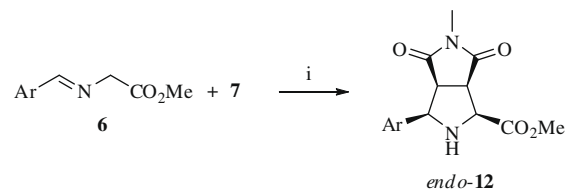
was surveyed. Several ester and aryl groups were appropriate substituents in iminoglycinates **6** to perform the 1,3-DC efficiently with NMM **11** (Scheme 2 and Table 3).

Non-substituted methyl aryliminoglycinates **6**, derived from benzaldehyde and 2-naphthalenecarbaldehyde, were the best substrates affording >99% ee (Table 3, entries 1, 2, and 6). In the example performed with catalytic complex (R)-**16**, the corresponding enantiomer (2S,3R,4R,5R)-endo-**12aa** was obtained (Table 3, entry 2). It was also demonstrated for these phenyl and 2-naphthyl derivatives that ethyl, isopropyl, and tert-butyl iminoglycinates were not suitable groups for obtaining the highest enantioselectivities (Table 3, entries 3, 4, 5, and 7). In these examples, it was also observed that larger amounts of the exo-diastereoisomer **12** were formed according to ^{1}H NMR spectroscopy and chiral HPLC. More sterically hindered iminoglycinates derived from ortho-substituted aromatic aldehydes gave lower enantioselectivity (Table 3, entries 8 and 9), even working at 0 or −20 °C and with bases other than Et$_3$N, such as DBU or DIEA. Using Et$_3$N as base, the imines derived from electron-donating or electron-withdrawing para-substituted aromatic aldehydes show a very similar tendency (Table 3, compare entries 11, 13, 14, and 16). In a few compounds, the ee was increased after recrystallization of the previously purified sample endo-**12fa** (Table 3, entry 13), but in other situations the employment of DBU as a base at 0 °C was crucial in order to achieve excellent enantioselectivity of endo-**12ea** and endo-**12ga** (Table 3,

Table 2
Recycling experiments of the 1:1 [(S)-Binap **8**]/AgClO$_4$ complex

Cycle	Reaction (mmol)	(S)-**6aa** (mmol)[a]	Recovered catalyst (%)	Yield (%)[b]	ee$_{endo}$ (%)[c]
1	1	0.100	95	91	>99
2	1	0.095[d]	93	89	>99
3	1	0.088[d]	92	91	>99
4	1	0.081[d]	90	90	99
5	1	0.073[d]	90	88	98

[a] Recovered after filtration of the crude reaction suspension and washed several times with toluene.
[b] Isolated yield of compound endo-**12aa** after recrystallization. The conversions were >99%, and the endo/exo ratio were >98:2 in all of the assayed cycles.
[c] Determined by chiral HPLC (Daicel Chiralpak AS).
[d] Amount recovered from the previous cycle.

Table 3
1.3-DC of iminoglycinates **6** and NMM **7**

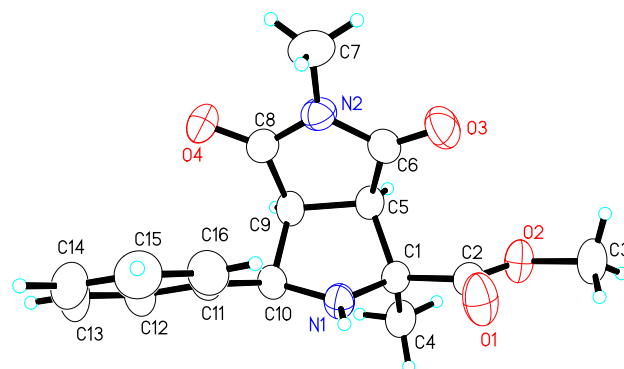| Entry	No	Ar	R	Base	Product endo-**12**			
					No.	Yield. (%)[a]	endo/exo[b]	ee$_{endo}$ (%)[c]
1	**6aa**	Ph	Me	Et$_3$N	**12aa**	90	>98:2	>99 (>99)[d]
2	**6aa**	Ph	Me	Et$_3$N	**12aa**[e]	90	>98:2	>99 (>99)[d]
3	**6ab**	Ph	Et	Et$_3$N	**12ab**	78	90:10	90 (91)
4	**6ac**	Ph	Pr^i	Et$_3$N	**12ac**	80	90:10	70 (72)
5	**6ad**	Ph	Bu^t	Et$_3$N	**12ad**	81	75:25	92 (92)
6	**6ba**	2-Naphthyl	Me	Et$_3$N	**12ba**	89	>98:2	99 (>99)[d]
7	**6bd**	2-Naphthyl	Bu^t	Et$_3$N	**12bd**	87	95:5	92 (94)
8	**6ca**	2-CH$_3$C$_6$H$_4$	Me	Et$_3$N	**12ca**	85[f]	>98:2	70 (75)
9	**6da**	2-ClC$_6$H$_4$	Me	Et$_3$N	**12da**	82[f]	>98:2	82 (85)
10	**6da**	2-ClC$_6$H$_4$	Me	Et$_3$N	**12da**	82[f,g]	>98:2	82 (85)
11	**6ea**	4-CH$_3$C$_6$H$_4$	Me	Et$_3$N	**12ea**	88	>98:2	86 (88)[d]
12	**6ea**	4-CH$_3$C$_6$H$_4$	Me	DBU	**12ea**	88	>98:2	99 (>99)[d]
13	**6fa**	4-(CH$_3$O)C$_6$H$_4$	Me	Et$_3$N	**12fa**	85	>98:2	80 (99)
14	**6fa**	4-(CH$_3$O)C$_6$H$_4$	Me	Et$_3$N	**12fa**	85[g]	>98:2	80 (99)
15	**6fd**	4-(CH$_3$O)C$_6$H$_4$	Bu^t	Et$_3$N	**12fd**	84	95:5	90 (91)
16	**6ga**	4-ClC$_6$H$_4$	Me	Et$_3$N	**12ga**	87	>98:2	64 (65)
17	**6ga**	4-ClC$_6$H$_4$	Me	DBU	**12ga**	87[g]	>98:2	98 (99)
18	**6gd**	4-ClC$_6$H$_4$	Bu^t	Et$_3$N	**12gd**	83	>98:2	80 (80)
19	**6ha**	2-Thienyl	Me	Et$_3$N	**12ha**	87	>98:2	90 (92)[h]
20	**6ha**	2-Thienyl	Me	Et$_3$N	**12ha**	87[g]	>98:2	90 (92)[h]

[a] Isolated yield after recrystallization.
[b] Determined by ^{1}H MNR.
[c] Determined by chiral HPLC (Chiralcel OD-H), the results of the recrystallized product are given in parentheses.
[d] Determined by chiral HPLC (Chiralpak AS).
[e] Molecule (2R.3S.4S.5S) endo-**12aa** obtained employing (R)-**16**.
[f] Purification by flash chromatography.
[g] Reaction performed with the recycled catalytic mixture.
[h] Determined by chiral HPLC (Chiralpak AD).

entries 12 and 17). Unlike the results described from phenyl and naphthyl derivatives the *tert*-butyl esters were more effective than the corresponding methyl esters in those examples containing a *para*-substituted aromatic residue imino group (compare entries 13 and 15, 16 and 18 of Table 3). Heteroaromatic iminoglycinate bearing a 2-thienyl group furnished *endo*-cycloadduct **12ha** with 92% ee after recrystallization (Table 3, entry 19). The recovery of

the complex (*S*)-**16** was successfully attempted in the examples recorded in entries 10, 14, and 20 of Table 3 in 88–93% yield by simple filtration.

Next, sterically hindered α-substituted benzaldimino esters were tested as substrates in the 1,3-DC with NMM. Methyl benzylidenealaninate **18**, methyl phenyliminophenylalaninate **19,** and methyl 2-thienyliminoleucinate **20** reacted with NMM under the same reaction conditions at room temperature for 48 h (Scheme 3). Cycloadducts *endo*-**21**–**23** were obtained diastereoselectively (>98:2 *endo/exo* ratio) and with good enantioselectivities (72–76% ee). However, compound *endo*-**22** was obtained after recrystallization in 98% ee, and in 58% yield (Scheme 3). The absolute configuration of the heterocycle (2R.3S.4S.5S) *endo*-**21** was determined by X-ray diffraction analysis (Fig. 4). 2-Thienyl derivatives *endo*-**12ha** and *endo*-**23** can be considered as structurally related precursors of active inhibitors of the virus that is responsible for hepatitis C **1** (Fig. 1).[11i,21]

Several maleimides were essayed employing the model reaction described in Scheme 1, which means benzyliminoglycinate **6aa**,
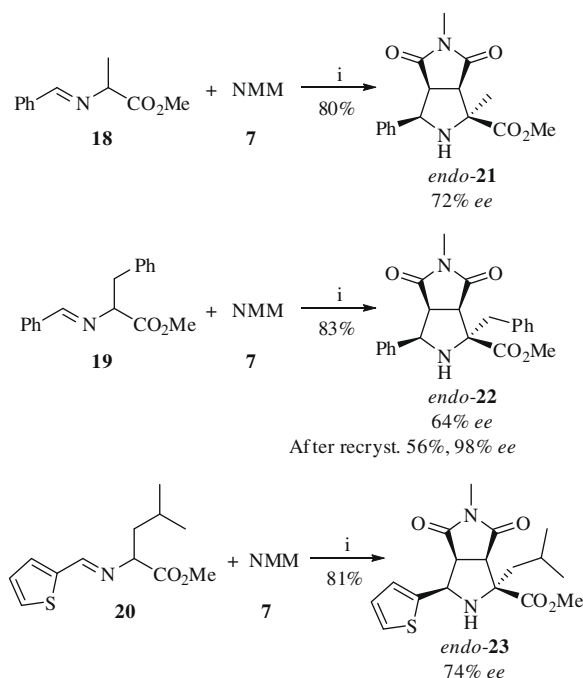
Scheme 3. Reagents and conditions: (i) (*S*)-Binap **8** (5 mol %), AgClO$_4$ (5 mol %), Et$_3$N (5 mol %), toluene, rt, 48 h.

Figure 4. ORTEP of cycloadduct *endo*-**21**.

endo-**12aa**

90%, >99% *ee*
endo:*exo* >98:2

endo-**24**

91%, >99% *ee*
endo:*exo* >98:2
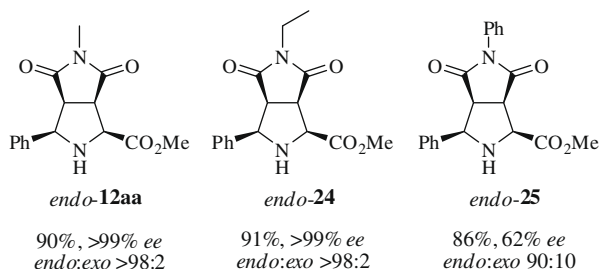
endo-**25**

86%, 62% *ee*
endo:*exo* 90:10

**Figure 5.** Products obtained from different *N*-substituted maleimides.

room temperature, (*S*)-**8** (5 mol %), AgClO₄ (5 mol %) and Et₃N (5 mol %) in toluene. *N*-Ethylmaleimide afforded similar results of *endo*-**24** to those analogous obtained with NMM **7** after 8 h of reaction (Fig. 5). Nevertheless, the bulkier *N*-phenylmaleimide (NPM) furnished a lower ee (62%) of *endo*-**25** and a lower diastereoselectivity (90:10 *endo*/*exo* ratio) (Fig. 5).

α-Monomethylated and α,β-dimethylated *N*-ethylmaleimides **26** and **29**, respectively, were prepared[22] and used as dipolarophiles. Non-symmetric maleimide **26** was an attractive reagent for studying the regioselectivity of this process. When the reaction was completed, cycloadducts **27** and **28** were obtained in a 44:56 ratio, respectively. This ratio remained unaltered when the reaction was run at 0 or at −20 °C, both in the presence of Et₃N or DBU. In general, better enantioselectivity was achieved with DBU (84 and 89% ee) (Scheme 4). However, no reaction was observed when 3,4-dimethyl-*N*-ethylmaleimide **29** was allowed to react with imino ester **6aa**.
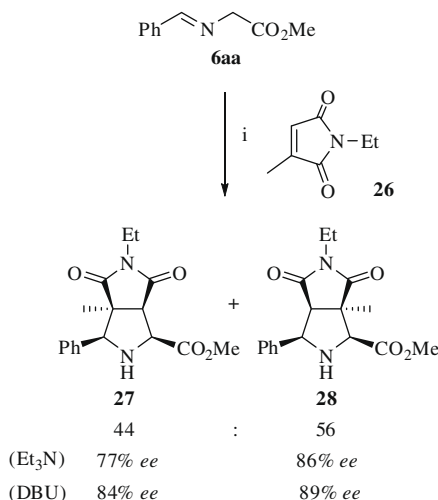
Scheme 4. Reagents and conditions: (i) (*S*)-Binap **8** (5 mol %), AgClO₄ (5 mol %), Et₃N (5 mol %), toluene, rt, 16 h.

Dipolarophiles other than maleimides were not appropriate for the particular requirements of this enantioselective 1,3-DC catalyzed by the in situ-generated complex (*S*)-**16** (Scheme 5 and Table
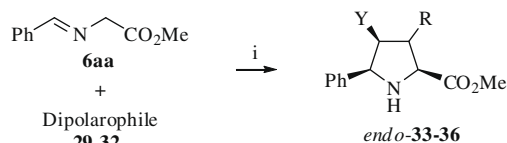
Scheme 5. (*S*)-Binap **8** (5 mol %), AgClO₄ (5 mol %), Et₃N (5 mol %), toluene, rt, 16 h.

4). Acrylates **29**, fumarates **30**, maleate **31**, and acrylonitrile **32** gave very high reaction conversions, but the enantioselectivities never exceeded of the 36% ee (Table 4) maintaining the high *endo*/*exo* diastereoselection. Maleic anhydride, nitrostyrene, acrylamide, and *N*-isopropylacrylamide did not react at all in spite of using DBU (10 mol %) as base or even other chiral ligands 9–11.
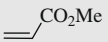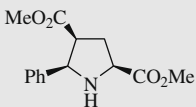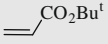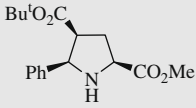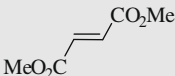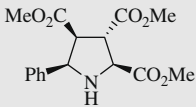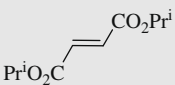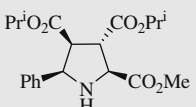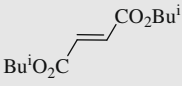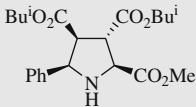
2.4. Computational studies

In order to get a better understanding of the behavior of these chiral catalysts, we have carried out DFT[23] calculations on the model reaction depicted in Scheme 1 and entry 7 of Table 1, using the DFT functional usually denoted as B3LYP.[24] Silver atoms were treated using the Hay and Wadt effective core potential and basis set[25] (denoted as LANL2DZ), whereas the remaining elements were described using the standard 6-31G* split-valence basis set.[26] All the calculations were carried out using the GAUSSIAN 03 suite of programs.[27] The graphics shown in Figures 6 and 7 were built up using the Maestro interface.[28] In the model systems **A–C,** we have included the cationic part of the presumed active complex (*S*)-**16** as well as a model azomethine ylide and maleimide **B**.

The chief geometric features of complex (*S*)-**A** are gathered in Figure 6. The azomethine ylide part of (*S*)-**A** shows different distances for the two C–N bonds. These distances are compatible with an iminium-enolate structure as shown in Scheme 6, thus anticipating quite asynchronous transition structures in the reaction with the dipolarophile. It is also observed that the metallic center is coordinated to the two phosphorus atoms of the catalysts and to the oxygen and nitrogen atoms of the azomethine ylide. This coordination pattern leads to the blockag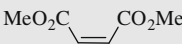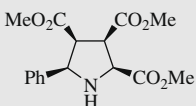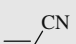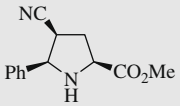e of the *Re* face of (*S*)-**A** by one of the phenyl groups of the phosphine unit (Fig. 6). This steric hindrance is also generated by the (*S*)-Binap moiety, in which the two α-naphthyl subunits form a dihedral angle of ca. 75°.

In previous work on chiral Ag-based catalysts we have observed a clear preference for the *endo*-cycloadducts because of the electrostatic interaction between the nitrogen atom of maleimide and the silver atom.[12e] Therefore, we considered the formation of the diastereomeric *endo*-cycloadducts **C** and **D** via transition structures **TS1** and **TS2**, respectively. The main geometric features and the relative energies of these transition structures are reported in Figure 7. It is found that the Gibbs activation energies are larger than the total activation energies because of the unfavorable entropic balance on going from the reactants to the saddle points, thus resulting in larger reaction times. As expected both **TS1** and **TS2** are quite asynchronous, **TS1** being ca. 2 kcal/mol more stable than **TS2**. In the latter transition structure, there is an appreciable steric clash between one of the phenyl groups of the phosphine moiety of (*S*)-**16** and the dipolarophile **B**. This results in a larger distortion of the (*S*)-**16** moiety in **TS2** with respect to (*S*)-**A**. As a result, exclusive formation of *endo*-(*S,S,S,R*)-**C** is predicted, in full agreement with the experimentally observed formation of cycloadducts *endo* described in the text. The same trend is found for the cycloadducts *endo*-(*S,S,S,R*)-**C** and *endo*-(*S,R,R,S*)-**D**, the latter being ca. 1.3 kcal/mol less stable than the former. Moreover, the slightly positive values of the Gibbs reaction energies associated with the formation of these catalyst-bound cycloadducts are compatible with the catalyst turnover since there is no inhibition of the catalyst by the product of the cycloaddition step. These calculations support that NMM is the best dipolarophile due to the coordination of the nitrogen atom to the metal center. On the other hand, the presence of a bulkier substituent in this nitrogen atom blocks the *endo*-approach reducing the enantioselectivity, such as that occurred with NPM. In summary, our calculations are in full agreement with the experimental findings and provide a rationale for the excellent asymmetric induction and catalytic efficiency of species similar to (*S*)-**16**.

Table 4
1,3-DC of iminoester 6aa with several dipolarophiles different to maleimides

Entry	Dipolarophile	No.	Structure	Product			
				No.	Yield[a] (%)	endo:exo[b]	ee$_{endo}$ (%)[c]
1	$\diagup$CO$_2$Me	**29a**	MeO$_2$C, Ph, N H, CO$_2$Me	**33a**	99	>98:2	30
2	$\diagup$CO$_2$Bu^t	**29d**	Bu^{t}O$_2$C, Ph, N H, CO$_2$Me	**33d**	99	>98:2	36
3	MeO$_2$C, CO$_2$Me	**30a**	MeO$_2$C, CO$_2$Me, Ph, N H, CO$_2$Me	**34a**	99	>98:2	28
4	Pr^{i}O$_2$C, CO$_2$Pr^i	**30c**	Pr^{i}O$_2$C, CO$_2$Pr^i, Ph, N H, CO$_2$Me	**34c**	99	>98:2	30
5	Bu^{i}O$_2$C, CO$_2$Bu^i	**30e**	Bu^{i}O$_2$C, CO$_2$Bu^i, Ph, N H, CO$_2$Me	**34e**	99	>98:2	36
6	MeO$_2$C, CO$_2$Me	**31a**	MeO$_2$C, CO$_2$Me, Ph, N H, CO$_2$Me	**35a**	99	>98:2	16
7	$\diagup$CN	**32**	NC, Ph, N H, CO$_2$Me	**36**	95	90:10	5

[a] Isolated crude yields.
[b] Determined by ^{1}H MNR.
[c] Determined by chiral HPLC (see Section 4).

3. Conclusions

By evaluating all the data described in the main text, we found that the employment of the complex generated by the 1:1 mixture of chiral Binap and AgClO$_4$ is very stable and can be manipulated without any special care. It was efficient in the catalyzed 1,3-DC using maleimides and aryliminoesters; however, other dipolarophiles did not work satisfactorily. The whole catalytic mixture can be recovered from the reaction mixture and reused without any loss of efficiency. The TS responsible for the enantiodiscrimination is, as expected, quite asynchronous, an appreciable steric clash between one of the phenyl groups of the phosphine moiety of (*S*)-**16** and the dipolarophile being the crucial interaction.

4. Experimental

4.1. General

All reactions were carried out in the absence of light. Anhydrous solvents were freshly distilled under an argon atmosphere. Aldehydes were also distilled prior to use for the elaboration of the iminoesters. Melting points were determined with a Reichert Thermovar hot plate apparatus and are uncorrected. Only the structurally most important peaks of the IR spectra (recorded on a Nicolet 510 P-FT) are listed. ^{1}H NMR (300 MHz) and ^{13}C NMR (75 MHz) spectra were obtained on a Bruker AC-300 using CDCl$_3$ as solvent and TMS as internal standard, unless otherwise stated. Optical rotations were measured on a Perkin Elmer 341 polarimeter. HPLC analyses were performed on a JASCO 2000-series equipped with a chiral column (detailed for each compound in the main text), using mixtures of *n*-hexane/isopropyl alcohol as mobile phase, at 25 °C. Low-resolution electron impact (EI) mass spectra were obtained at 70 eV on a Shimadzu QP-5000, and high-resolution mass spectra were obtained on a Finnigan VG Platform. HRMS (EI) were recorded on a Finnigan MAT 95S. Microanalyses were performed on a Perkin Elmer 2400 and a Carlo Erba EA1108. Analytical TLC was performed on Schleicher & Schuell F1400/LS silica gel plates, and the spots were visualized under UV light (λ = 254 nm). For flash chromatography, we employed Merck silica gel 60 (0.040–0.063 mm).

4.2. 1,3-Dipolar cycloaddition of iminoesters 6 and dipolarophiles. General procedure

A solution of the imino ester (1 mmol) and dipolarophile (1 mmol) in toluene (5 mL) was added to a suspension containing (*R*)- or (*S*)-Binap (0.05 mmol, 31 mg) and AgClO$_4$ (0.05 mmol, 10 mg) in toluene (5 mL). To the resulting suspension, triethylamine (0.05 mmol, 7 µL) was added, and the mixture stirred at room temperature and in the absence of the light for 16–48 h (see main text). The precipitate was filtered, and the complex
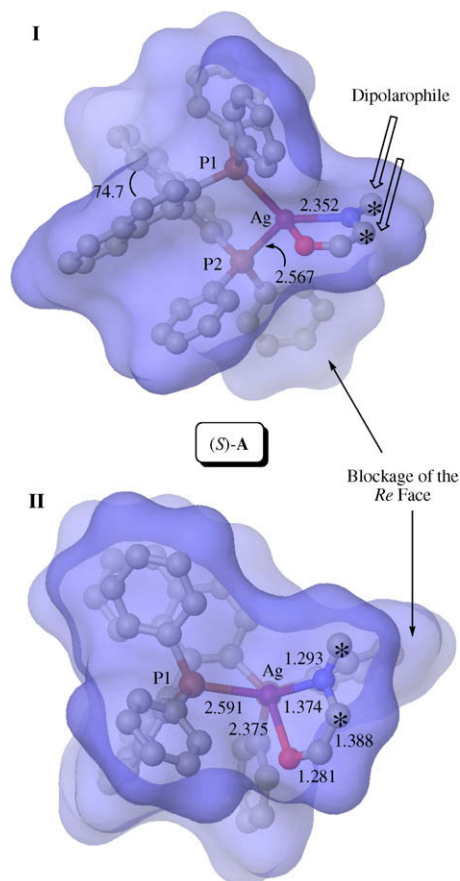
Figure 6. (I) Fully optimized structure (B3LYP/LANL2DZ&6-31G* level) of (S)-**A**. The hydrogen atoms have been omitted for clarity. The carbon atoms of the azomethine ylide moiety have been highlighted with asterisks. Bond distances and dihedrals are given in Å and deg., respectively. The molecular surface (Probe radius: 1.4 Å) is also included. (II) View over the Si face of (S)-**A** along the axis determined by the Ag and P2 atoms.
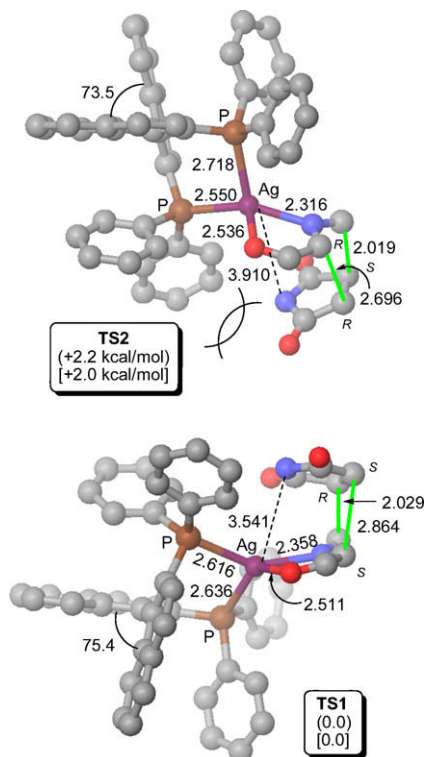
Figure 7. Fully optimized structure (B3LYP/LANL2DZ&6-31G* level) of **TS1** and **TS2** leading to endo-(S,S,R)-**C** and endo-(S,R,R,S)-**D**, respectively. The hydrogen atoms have been omitted for clarity. Bond distances and dihedrals are given in Å and °, respectively. Numbers in parentheses and in square brackets are the relative total and Gibbs free energies respectively, computed at the B3LYP/LANL2DZ&6-31G*+ΔZPVE level.

was recovered. The organic filtrate was directly evaporated, and the residue was purified by recrystallization or by flash chromatography yielding pure endo-cycloadducts.

The solid was washed with warm toluene twice, and then dissolved in DCM in order to transfer the catalytic complex into the
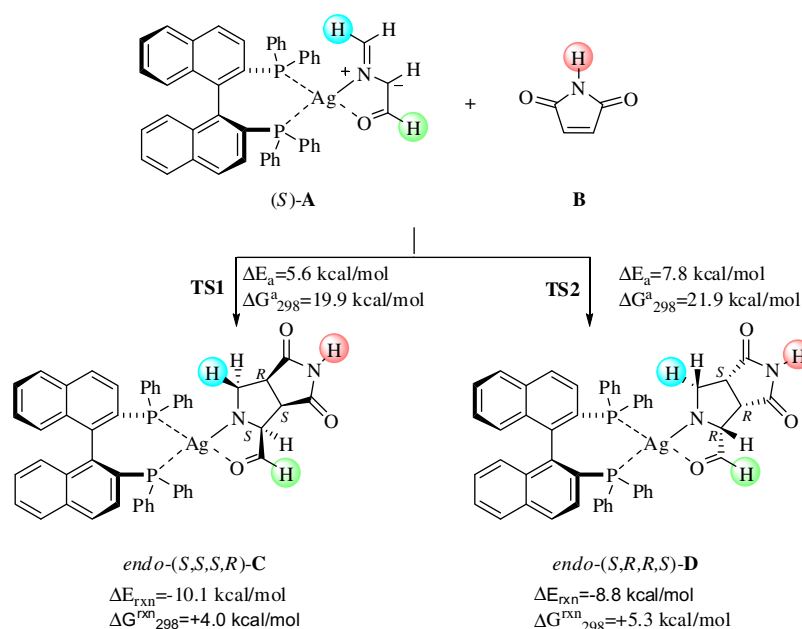
Scheme 6. Model reaction used in the computational studies. The hydrogen atoms highlighted in blue, green and red correspond to a phenyl, a methoxy and a methyl group respectively in the reaction depicted in Scheme 1.

flask. After evaporation of DCM, the resulting solid was ready to catalyze a new batch.

4.2.1. Methyl (1*S*,3*R*,3a*S*,6a*R*)-5-methyl-3-phenyl-4,6-dioxoocta-hydropyrrolo[3,4-*c*]pyrrole-1-carboxylate 12aa[12a,19]

4.2.2. Ethyl (1*S*,3*R*,3a*S*,6a*R*)-5-methyl-3-phenyl-4,6-dioxooctahydropyrrolo[3,4-*c*]pyrrole-1-carboxylate 12ab

Colorless prisms, mp, 195–197 °C (CH$_2$Cl$_2$/hex); $[\alpha]_D^{20}$ = +74 (*c* 1, CHCl$_3$, 90% ee from HPLC); R_f: 0.36 (*n*-hexane/ethyl acetate: 1/5); IR (KBr) *v*: 1752, 1702, 3325 cm^{-1}; ^{1}H NMR δ_H: 1.38 (t, *J* = 7.1 Hz, 3H, CO$_2$CH$_2$C*H$_3$), 2.41 (br s, 1H, NH), 2.85 (s, 3H, NCH$_3$), 3.41 (dd, *J* = 8.2, 8.0 Hz, 1H, C*H*CHAr), 3.55 (dd, *J* = 7.3, 7.1 Hz, 1H, CHC*H*CO$_2$Et), 4.01 (d, *J* = 5.7 Hz, 1H, C*H*CO$_2$CH$_3$), 4.32 (m, 2H, CO$_2$C*H$_2$CH$_3$), 4.47 (d, *J* = 8.1 Hz, 1H, CHPh), 7.28–7.36 (m, 5H, ArH); ^{13}C NMR δ_C: 14.1 (CO$_2$CH$_2$*C*H$_3$), 24.9 (NCH$_3$), 48.1, 49.5 (2CHCON), 61.3 (CO$_2$*C*H$_2$CH$_3$), 61.7 (*C*HCO$_2$Et), 63.9 (Ph–CH), 126.9, 128.2, 128.3 (ArCH), 136.7 (ArC), 169.6, 174.7, 175.8 (CO$_2$Me and CON); MS (EI) *m/z* (%): 302 (M$^+$, 3.90%), 230 (16), 229 (100), 191 (37), 144 (37), 117 (43); HRMS calcd for C$_{16}$H$_{18}$N$_2$O$_4$: 302.1267, found: 302.1292; Microanalysis calcd for C$_{16}$H$_{18}$N$_2$O$_4$: C, 63.5; H, 6.0; N, 9.2. Found: C, 63.5; H, 5.7; N, 9.1. HPLC (Chiralcel OD-H, 1 mL/min, *n*-hexane/*i*-PrOH: 80/20, λ 215 nm), t_{Rmaj} = 24.1 min, t_{Rmin} = 25.8 min.

4.2.3. Isopropyl (1*S*,3*R*,3a*S*,6a*R*)-5-methyl-3-phenyl-4,6-dioxooctahydropyrrolo[3,4-*c*]pyrrole-1-carboxylate 12ac

Colorless prisms, mp, 202 °C (CH$_2$Cl$_2$/hex); $[\alpha]_D^{20}$ = +63 (*c* 0.7, CHCl$_3$, 99% ee from HPLC); R_f: 0.50 (*n*-hexane/ethyl acetate: 1/5); IR (KBr) *v*: 1735, 1703, 3328 cm^{-1}; ^{1}H NMR δ_H: 1.33 [d, *J* = 6.2 Hz, 3H, CO$_2$CH(C*H$_3$)$_2$], 1.41 [d, *J* = 6.3 Hz, 3H, CO$_2$CH(C*H$_3$)$_2$], 2.42 (br s, 1H, NH), 2.87 (s, 3H, NCH$_3$), 3.43 (dd, *J* = 8.3, 8.0 Hz, 1H, C*H*CHPh), 3.56 (dd, *J* = 7.2, 7.1 Hz, 1H, CHC*H*CO$_2$Pr^i), 4.00 (dd, *J* = 6.7, 5.7 Hz, 1H, C*H*CO$_2$Pr^i), 4.49 (dd, *J* = 8.4, 5.8 Hz, 1H, CHPh), 5.22 [m, 1H, CO$_2$C*H*(CH$_3$)$_2$], 7.29–7.40 (m, 5H, ArH); ^{13}C NMR δ_C: 21.6, 21.9 [CO$_2$CH(*C*H$_3$)$_2$], 24.9 (NCH$_3$), 48.2, 49.7 (2CHCON), 62.0 [CO$_2$*C*H(CH$_3$)$_2$], 64.0 (*C*HCO$_2$Pr^i), 69.3 (Ph–CH), 126.6, 128.3, 128.4 (ArCH), 136.6 (ArC), 169.1, 174.8, 175.8 (CO$_2$Me and CON); MS (EI) *m/z* (%): 316 (M$^+$, 2.23%), 230 (15), 229 (100), 205 (14), 144 (29), 117 (19); HRMS calcd for C$_{17}$H$_{20}$N$_2$O$_4$: 316.1423, found: 316.1426; Microanalysis calcd for C$_{17}$H$_{20}$N$_2$O$_4$: C, 64.5; H, 6.3; N, 8.8. Found: C, 64.5; H, 6.3; N, 8.5. HPLC (Chiralcel OD-H, 1 mL/min, *n*-hexane/*i*-PrOH: 80/20, λ 215 nm), t_{Rmaj} = 21.5 min, t_{Rmin} = 33.4 min.

4.2.4. *tert*-Butyl (1*S*,3*R*,3a*S*,6a*R*)-5-methyl-3-phenyl-4,6-dioxooctahydropyrrolo[3,4-*c*]pyrrole-1-carboxylate 12ad

Colorless prisms, mp, 210 °C (subl.) (CH$_2$Cl$_2$/hex); $[\alpha]_D^{20}$ = +33.9 (*c* 0.8, CHCl$_3$, 92% ee from HPLC); R_f: 0.39 (*n*-hexane/ethyl acetate: 1/5); IR (KBr) *v*: 1734, 1705, 3328 cm^{-1}; ^{1}H NMR δ_H: 1.58 [s, 9H, CO$_2$C(C*H$_3$)$_3$], 2.40 (br s, 1H, NH), 2.86 (s, 3H, NCH$_3$), 3.42 (dd, *J* = 8.2, 8.1 Hz, 1H, C*H*CHPh), 3.54 (dd, *J* = 7.2, 7.1 Hz, 1H, CHC*H*CO$_2$Bu^t), 3.94 (m, 1H, C*H*CO$_2$Bu^t), 4.49 (dd, *J* = 8.5, 6.1 Hz, 1H, CHPh), 7.26–7.36 (m, 5H, ArH); ^{13}C NMR δ_C: 24.9 (NCH$_3$), 28.1 [CO$_2$C(*C*H$_3$)$_3$], 48.2, 49.8 (2CHCON), 62.4 (*C*HCO$_2$Bu^t), 63.8 (Ph–CH), 82.5 [CO$_2$*C*(CH$_3$)$_3$], 126.6, 128.2, 128.4 (ArCH), 136.7 (ArC), 174.8, 175.8 (CON); MS (EI) *m/z* (%): 330 (M$^+$, 0.01%), 230 (18), 229 (100), 144 (25) 117 (18); HRMS calcd for C$_{18}$H$_{22}$N$_2$O$_4$: 330.1580, found: 229.0986; Microanalysis calcd for C$_{18}$H$_{22}$N$_2$O$_4$: C, 65.4; H, 6.7; N, 8.5. found: C, 65.4; H, 6.6; N, 8.3. HPLC (Chiralcel OD-H, 1 mL/min, *n*-hexane/*i*-PrOH: 70/30, λ 215 nm), t_{Rmaj} = 12.1 min, t_{Rmin} = 17.3 min.

4.2.5. Methyl (1*S*,3*R*,3a*S*,6a*R*)-5-methyl-3-(2-naphthyl)-4,6-dioxooctahydropyrrolo[3,4-*c*]pyrrole-1-carboxylate 12ba[11h]

4.2.6. *tert*-Butyl (1*S*,3*R*,3a*S*,6a*R*)-5-methyl-3-(2-naphthyl)-dioxooctahydropyrrolo[3,4-*c*]pyrrole-1-carboxylate 12bd

Colorless prisms, mp, 150-152 °C (CH$_2$Cl$_2$/hex); $[\alpha]_D^{20}$ = +39.8 (*c* 1, CHCl$_3$, 92% ee from HPLC, 75:25 *endo/exo*); R_f: 0.46 (*n*-hexane/

ethyl acetate: 1/5); IR (KBr) *v*: 1715, 1689, 1678, 3341 cm^{-1}; ^{1}H NMR δ_H: 1.32 [s, 9H, CO$_2$C(C*H$_3$)$_3$], 2.29 (br s, 1H, NH), 3.05 (s, 3H, NCH$_3$), 3.56 (m, 1H, C*H*CHAr), 3.86 (m, 1H, CHC*H*CO$_2$CH$_3$), 4.00 (d, *J* = 4.2 Hz, 1H, C*H*CO$_2$CH$_3$), 4.65 (d, *J* = 4.9 Hz, 1 H, CHAr), 7.40-7.49 (m, 3H, ArH), 7.80-7.86 (m, 4H, ArH); ^{13}C NMR δ_C: 25.2 (NCH$_3$), 27.7 [CO$_2$C(*C*H$_3$)$_3$].48.2, 49.1, 52.0 (2CHCON and CO$_2$CH$_3$), 63.3 (*C*HCO$_2$Bu^t), 65.3 (2-Napht–CH), 82.6 [CO$_2$*C*(CH$_3$)$_3$], 124.8, 125.2, 126.2, 126.4, 127.6, 128.0, 128.7 (ArCH), 133.0, 133.3 137.9 (ArC), 170.4, 176.9, 177.1 (CO$_2$ Bu^t and CON); MS (EI) *m/z* (%): 380 (M$^+$, 1.78%), 280 (18), 279 (100), 194 (22), 167 (13); HRMS calcd for C$_{22}$H$_{24}$N$_2$O$_4$: 380.1736, found: 380.1725; Microanalysis calcd for C$_{22}$H$_{24}$N$_2$O$_4$: C, 69.5; H, 6.4; N, 7.4. found: C, 69.5; H, 6.3; N, 7.1. HPLC (Chiralcel OD-H, 1 mL/min, *n*-hexane/*i*-PrOH: 70/30, λ 225 nm), t_{Rmaj} = 13.5 min, t_{Rmin} = 22.0 min.

4.2.7. Methyl (1*S*,3*R*,3a*S*,6a*R*)-5-methyl-4,6-dioxo-3-*o*-tolyloctahydropyrrolo[3,4-*c*]pyrrole-1-carboxylate 12ca

Colorless prisms, mp, 151 °C (CH$_2$Cl$_2$/hex); $[\alpha]_D^{20}$ = 50.8 (*c* 0.6, CHCl$_3$, 75% ee from HPLC); R_f: 0.25 (*n*-hexane/ethyl acetate: 1/5); IR (KBr) *v*: 1768, 1734, 1698, 2954 cm^{-1}; ^{1}H NMR δ_H: 2.35 (s, 3H, ArCH$_3$), 2.75 (s, 3H, NCH$_3$), 3.46 (m, 1H, C*H*CHAr), 3.67 (m, 1H, CHC*H*CO$_2$CH$_3$), 3.82 (s, 3H, CO$_2$CH$_3$), 3.99 (d, *J* = 6.2 Hz, 1H, C*H*CO$_2$CH$_3$), 4.54 (d, *J* = 8.1 Hz, 1H, CHAr), 7.08-7.15 (m, 3H, ArH), 7.36-7.39 (m, 1H, ArH); ^{13}C NMR δ_C: 19.4 (ArCH$_3$), 24.9 (NCH$_3$), 46.9, 48.0, 52.3 (2CHCON and CO$_2$CH$_3$), 61.2 (*C*HCO$_2$Me), 67.9 (2-MePh–CH), 125.1, 126.1, 127.8, 130.1 (ArCH), 135.2, 135.5 (ArC), 170.2, 174.4, 176.1 (CO$_2$Me and CON); MS (EI) *m/z* (%): 302 (M$^+$, 15.36%), 243 (67), 244 (10), 193 (10), 192 (85), 191 (78), 160 (28), 159 (11), 158 (38), 132 (38), 131 (100), 130 (36), 118 (15), 115 (14), 105 (20), 104 (11), 103 (13), 91 (15), 77 (11); HRMS calcd for C$_{16}$H$_{18}$N$_2$O$_4$: 302.1267, found: 302.1247; Microanalysis calcd for C$_{16}$H$_{18}$N$_2$O$_4$: C, 63.6; H, 6.0; N, 9.3. found: C, 63.6; H, 6.3; N, 9.0. HPLC (Chiralcel OD-H, 1 mL/min, *n*-hexane/*i*-PrOH: 70/30, λ 225 nm), t_{Rmin} = 24.7 min, t_{Rmaj} = 28.1 min.

4.2.8. Methyl (1*S*,3*R*,3a*S*,6a*R*)-3-(2-chlorophenyl)-5-methyl-4,6-dioxooctahydropyrrolo[3,4-*c*]pyrrole-1-carboxylate 12da[11h]

4.2.9. Methyl (1*S*,3*R*,3a*S*,6a*R*)-5-methyl-3-(4-methylphenyl)-4,6-dioxooctahydropyrrolo[3,4-*c*]pyrrole-1-carboxylate 12ea[11h]

4.2.10. Methyl (1*S*,3*R*,3a*S*,6a*R*)-3-(4-methoxyphenyl)-5-methyl-4,6-dioxooctahydropyrrolo[3,4-*c*]pyrrole-1-carboxylate 12fa[11h]

4.2.11. *tert*-Butyl (1*S*,3*R*,3a*S*,6a*R*)-3-(4-methoxyphenyl)-5-methyl-4,6-dioxooctahydropyrrolo[3,4-*c*]pyrrole-1-carboxylate 12fd

Colorless prisms, mp, 179 °C (CH$_2$Cl$_2$/hex); $[\alpha]_D^{20}$ = +93 (*c* 0.5, CHCl$_3$, 84% ee from HPLC); R_f: 0.29 (*n*-hexane/ethyl acetate: 1/5); IR (KBr) *v*: 1702, 1733, 2977 cm^{-1}; ^{1}H NMR δ_H: 1.58 [s, 9H, CO$_2$C(C*H$_3$)$_3$], 1.86 (br s, 1H, NH), 2.88 (s, 3H, NCH$_3$), 3.38 (dd, *J* = 8.2, 8.0 Hz, 1H, C*H*CHAr), 3.53 (dd, *J* = 7.1, 7.0 Hz, 1H, CHC*H*CO$_2$Bu^t), 3.80 (s, 3H, OCH$_3$), 3.92 (d, *J* = 6.7 Hz, 1H, C*H*CO$_2$Bu^t), 4.43 (d, *J* = 8.6 Hz, 1H, CHAr), 6.87 (d, *J* = 8.7 Hz, 2H, ArH), 7.24 (d, *J* = 8.7 Hz, 2H, ArH); ^{13}C NMR δ_C: 24.9 (NCH$_3$), 28.1 [CO$_2$C(*C*H$_3$)$_3$], 48.2, 49.7 (2CHCON), 55.1 (OCH$_3$), 62.3 (*C*HCO$_2$Bu^t), 63.4 (4-MeOPh–CH), 82.5 [CO$_2$*C*(CH$_3$)$_3$], 113.7, 128.1 (ArCH), 159.3, 168.6 (ArC), 175.1, 175.9 (CON); MS (EI) *m/z* (%): 360 (M$^+$, 4.15%), 260 (15), 259 (100), 249 (12), 193 (45), 174 (24), 147 (29); HRMS calcd for C$_{19}$H$_{24}$N$_2$O$_5$: 360.1685, found: 360.1674; Microanalysis calcd for C$_{19}$H$_{24}$N$_2$O$_5$: C, 63.3; H, 6.7; N, 7.7. found: C, 63.5; H, 6.6; N, 7.4. HPLC (Chiralpak AS, 1 mL/min, *n*-hexane/*i*-PrOH: 90/10, λ 205 nm), t_{Rmin} = 25.2 min, t_{Rmaj} = 43.7 min.

4.2.12. Methyl (1*S*,3*R*,3a*S*,6a*R*)-3-(4-chlorophenyl)-5-methyl-4,6-dioxooctahydropyrrolo[3,4-*c*]pyrrole-1-carboxylate 12ga[11h]

4.2.13. *tert*-Butyl (1*S*,3*R*,3a*S*,6a*R*)-3-(4-chlorophenyl)-5-methyl-4,6-dioxooctahydropyrrolo[3,4-*c*]pyrrole-1-carboxylate 12gd

Colorless prisms, mp, 129-131 °C (CH$_2$Cl$_2$/hex); $[\alpha]_D^{20}$ = +16 (*c* 0.5, CHCl$_3$, 82% ee from HPLC); R_f: 0.36 (*n*-hexane/ethyl acetate:

1/5); IR (KBr) ν: 1729, 1708, 3328 cm^{-1}; ^{1}H NMR δ_H: 1.57 [s, 9H, CO$_2$C(CH_3)$_3$], 2.39 (br s, 1H, NH), 2.84 (s, 3H, NCH_3), 3.41 (dd, J = 8.2, 8.1 Hz, 1H, CHCHAr), 3.54 (dd, J = 7.6, 6.9 Hz, 1H, CHCHCO$_2$-Bu^t), 3.95 (dd, J = 6.4, 5.7 Hz, 1H, CHCO$_2$Bu^t), 4.45 (dd, J = 8.6, 5.8 Hz, 1H, CHAr), 7.24–7.31 (m, 5 H, ArH); ^{13}C NMR δ_C: 24.9 (NCH_3), 28.0 [CO$_2$C(CH_3)$_3$], 47.8, 49.4 (2CHCON), 62.2 (CHCO$_2$Bu^t), 63.0 (*p*-Cl–CH), 82.6 [CO_2C(CH$_3$)$_3$], 128.3, 128.6 (ArCH), 133.9, 135.3 (ArC), 174.6, 175.6 (CON); MS (EI) *m/z* (%): 364 (M$^+$, 0.21%), 265 (32), 264 (15), 263 (100), 178 (21), 151 (10), 143 (11), 57 (12); HRMS calcd for C$_{18}$H$_{21}$ClN$_2$O$_4$: 364.1190, found: 364.1207; Microanalysis calcd for C$_{18}$H$_{21}$ClN$_2$O$_4$: C, 59.3; H, 5.8; N, 7.7. found: C, 59.1; H, 5.8; N, 7.4. HPLC (Chiralcel OD-H, 1 mL/min, *n*-hexane/*i*-PrOH: 80/20, λ 215 nm), t_{Rmaj} = 14.5 min, t_{Rmin} = 26.5 min.

4.2.14. Methyl (1*S*,3*R*,3a*S*,6a*R*)-5-methyl-4,6-dioxo-3-(2-thienyl)octahydropyrrolo[3,4-*c*]pyrrole-1-carboxylate 12ha[11h]
4.2.15. Methyl (1*S*,3*R*,3a*S*,6a*R*)-1,5-dimethyl-4,6-dioxo-3-phenyloctahydropyrrolo[3,4-*c*]pyrrole-1-carboxylate 21[11h]
4.2.16. Methyl (1*S*,3*R*,3a*S*,6a*R*)-1-benzyl-5-methyl-4,6-dioxo-3-phenyloctahydropyrrolo[3,4-*c*]pyrrole-1-carboxylate 22[11h]
4.2.17. Methyl (1*S*,3*R*,3a*S*,6a*R*)-1-isobutyl-5-methyl-4,6-dioxo-3-(2-thienyl)octahydropyrrolo[3,4-*c*]pyrrole-1-carboxylate 23[11h]
4.2.18. Methyl (1*S*,3*R*,3a*S*,6a*R*)-5-ethyl-3-phenyl-4,6-dioxooctahydropyrrolo[3,4-*c*]pyrrole-1-carboxylate 24[12a,19]
4.2.19. Methyl (1*S*,3*R*,3a*S*,6a*R*)-3,5-diphenyl-4,6-dioxooctahydropyrrolo[3,4-*c*]pyrrole-1-carboxylate 25[12a,19]
4.2.20. Methyl (1*S*,3*R*,3a*S*,6a*R*)-5-ethyl-3a-methyl-3-phenyl-4,6-dioxooctahydropyrrolo[3,4-*c*]pyrrole-1-carboxylate 27

(Isolated together isomer **28**): ^{1}H NMR δ_H:1.09 (t, J = 7.2 Hz, 3H, NCH$_2$CH_3), 1.49 (s, 3H, CCH_3), 2.39 (br s, 1H, NH), 3.12 (d, J = 6.4 Hz, 1H, CHCHCO$_2$CH$_3$), 3.43 (m, 2H, NCH_2CH$_3$), 3.87 (s, 3H, CO$_2$CH_3), 4.00 (br s, 1H, CHPh), 4.07 (d, J = 4.4, Hz, 1H, CHCO$_2$CH$_3$), 7.32–7.34 (m, 4H, ArH); ^{13}C NMR δ_C: 13.1 (CH$_2$CH_3), 20.0 (CCH_3), 33.9 (CH_2CH), 52.2 (CO$_2$CH_3), 54.5 (CHCON), 54.6 (CCH$_3$), 60.4 (CHCO$_2$Me), 71.9 (Ph–CH), 126.9, 128.2, 128.5 (ArCH), 136.6, 136.9 (ArC), 170.2, 173.9, 175.1 (CO$_2$Me and CON).

4.2.21. Methyl (1*S*,3*R*,3a*S*,6a*R*)-5-ethyl-6a-methyl-3-phenyl-4,6-dioxooctahydropyrrolo[3,4-*c*]pyrrole-1-carboxylate 28

(Isolated together isomer **27**). ^{1}H NMR δ_H:1.09 (t, J = 7.2 Hz, 3H, NCH$_2$CH_3), 1.60 (s, 3H, CCH_3), 2.39 (br s, 1H, NH), 2.98 (d, J = 8.4 Hz, 1H, CHCHPh), 3.43 (m, 2H, NCH_2CH$_3$), 3.71 (d, J = 3.4 Hz, 1H, CHCO$_2$CH$_3$), 3.87 (s, 3H, CO$_2$CH_3), 4.53 (dd, J = 8.2, 4.1 Hz, 1H, CHAr), 7.32–7.34 (m, 4H, ArH); ^{13}C NMR δ_C: 13.1 (CH$_2$CH_3), 20.0 (CCH_3), 33.9 (CH_2CH), 52.2 (CO$_2$CH_3), 54.6 (CCH$_3$), 56.9 (CHCON), 63.0 (Ph–CH), 68.2 (CHCO$_2$Me), 126.9, 128.2, 128.5 (ArCH), 136.6, 136.9 (ArC), 170.2, 177.3, 178.7(CO$_2$Me and CON).

4.2.22. Dimethyl (2*S*,4*S*,5*R*)-5-phenylpyrrolidine-2,4-dicarboxylate 33a[11b]
4.2.23. 4-*tert*-Butyl 2-methyl (2*S*,4*S*,5*R*)-5-phenylpyrrolidine-2,4-dicarboxylate 33b[11b]
4.2.24. Trimethyl (2*S*,3*S*,4*S*,5*R*)-5-phenylpyrrolidine-2,3,4-tricarboxylate 34a[12a,19]

4.2.25. 3,4-Diisopropyl (2*S*,3*S*,4*S*,5*R*)-2-methyl-5-phenylpyrrolidine-2,3,4-tricarboxylate 34c

Sticky oil; $[\alpha]_D^{20}$ = +32.1 (*c* 0.5, CHCl$_3$.82% ee from HPLC); R_f: 0.37 (*n*-hexane/ethyl acetate: 3/2); IR (liq.) ν: 1741, 1731, 2982 cm^{-1}; ^{1}H NMR δ_H: 0.65 [d, J = 6.2 Hz, 3H, CH(CH_3)$_2$], 0.94 [d, J = 6.2 Hz, 3H, CH(CH_3)$_2$], 1.27 [d, J = 6.2 Hz, 3H, CH(CH_3)$_2$], 1, 28 [d, J = 6.2 Hz, 3H, CH(CH_3)$_2$], 2.86 (br s, 1H, NH), 3.55 (m, 2H, 2 × HCO$_2$Pr^i), 3.83 (s, 3H, CO$_2$CH_3), 4.14 (d, J = 7.3 Hz, 1H, CHCO$_2$Me), 4.56 [sept, J = 6.2 Hz, 1H, CH(CH$_3$)$_2$], 4.65 (d, J = 7.3 Hz, 1H, CH-Ph), 5.08 [sept, J = 6.2 Hz, 1H, CH(CH$_3$)$_2$], 7.22–7.34 (m, 5H, ArH); ^{13}C NMR δ_C: 20.8, 21.4, 21.6 [CH(CH_3)$_2$], 51.4,

52.4 (CHCO$_2$Pr^i), 53.8 (CO$_2$CH$_3$), 63.4 [CHCO$_2$Me], 65.2 (Ph-CH), 68.2, 68.8 [CH(CH$_3$)$_2$], 127.0, 127.7, 128.2 (ArCH), 138.4 (ArC), 170.5, 171.5, 171.6 (CO$_2$Me, CO$_2$Pr^i); MS (EI) *m/z* (%): 377 (M$^+$, 13.84%), 318 (33), 317 (23), 316 (23), 290 (20), 276 (17), 274 (12), 258 (38), 248 (15), 230 (43), 228 (17), 216 (10), 205 (25), 202 (50), 188 (47), 187 (23), 177 (67), 170 (34), 149 (12), 146 (29), 145 (46), 144 (100), 143 (29), 119 (22), 118 (19), 117 (96), 116 (14), 115 (28), 106 (11), 104 (10), 91 (12), 90 (10); HRMS calcd for C$_{20}$H$_{27}$NO$_6$: 377.1838, found: 377.1863; HPLC (Chiralcel OD-H, 1 mL/min, *n*-hexane/*i*-PrOH: 80:20, λ 220 nm), t_{Rmaj} = 6.6 min, t_{Rmin} = 13.5 min.

4.2.26. 3,4-Diisobutyl 2-methyl (2*S*,3*S*,4*S*,5*R*)-5-phenylpyrrolidine-2,3,4-tricarboxylate 35e

Sticky oil; $[\alpha]_D^{20}$ = +47.1 (*c* 0.5, CHCl$_3$.82% ee from HPLC); R_f: (*n*-hexane/ethyl acetate: 1/5); IR (liq.) ν: 1737, 1730, 2958 cm^{-1}; ^{1}H NMR δ_H: 0.66 [d, J = 6.7 Hz, 3H, CH(CH_3)$_2$], 0.68 [d, J = 6.6 Hz, 3H, CH(CH_3)$_2$], 0.95 [d, J = 6.7 Hz, 6H, CH(CH_3)$_2$], 1.51 [d, J = 6.7 Hz, 1H, CH(CH$_3$)$_2$], 1.63 (br s, 1H, NH), 1.97 [d, J = 6.7 Hz, 1H, CH(CH$_3$)$_2$], 3.25 [dd, J = 10.5, 6.6 Hz, 1H, CH_2CH(CH$_3$)$_2$], 3.50 [dd, J = 10.6, 6.6 Hz, 1H, CH_2CH(CH$_3$)$_2$], 3.63 (m, 2H, 2 × CHCO$_2$Bu^i), 3.83 (s, 3H, CO$_2$CH_3), 3.96 [m, 2H, CH_2CH(CH$_3$)$_2$], 4.19 (d, J = 7.3 Hz, 1H, CHCO$_2$Me), 4.66 (d, J = 7.5 Hz, 1H, CH-Ph), 7.25–7.32 (m, 5H, ArH); ^{13}C NMR δ_C: 18.8, 18.9, 19.0 [CH(CH_3)$_2$], 27.2, 27.7 [CH(CH$_3$)$_2$], 51.3 (CHCO$_2$Bu^i), 52.5 (CO$_2$CH_3), 54.0 (CHCO$_2$Bu^i), 63.4 [CHCO$_2$Me], 65.5 (Ph–CH), 71.1, 71.5 (CH$_2$), 126.9, 127.8, 128.3 (ArCH), 138.1 (ArC), 171.4, 172.1, 172.2 (CO$_2$Me, CO$_2$Bu^i); MS (EI) *m/z* (%): 405 (M$^+$, 10.61%), 346 (11), 345 (22), 332 (20), 304 (20), 272 (36), 245 (11), 244 (54), 219 (11), 202 (38), 188 (38), 178 (11), 177 (90), 170 (26), 164 (46), 155 (12).149 (14), 146 (54), 145 (46), 144 (82), 143 (24), 119 (12), 118 (19), 117 (100), 116 (13), 115 (21), 106 (11), 105 (11), 90 (11), 57 (46), 56 (21), 55 (12); HRMS calcd for C$_{22}$H$_{31}$NO$_6$: 405.2151, found: 405.2171; HPLC (Chiralcel OD-H, 1 mL/min, *n*-hexane/*i*-PrOH: 80:20, λ 220 nm), t_{Rmaj} = 8.5 min, t_{Rmin} = 16.7 min.

4.2.27. Trimethyl (2*S*,3*R*,4*S*,5*R*)-5-phenylpyrrolidine-2,3,4-tricarboxylate 35a[12a,19]
4.2.28. Methyl (2*S*,4*S*,5*R*)-4-cyano-5-phenylpyrrolidine-2-carboxylate 36[29]

Acknowledgments

References

1. Karoyan, P.; Sagan, S.; Lequin, O.; Cluancard, J.; Lavielle, S.; Chassaing, G. *Targets Heterocycl. Syst.* **2004**, *8*, 216–273.
2. Pujals, S.; Giralt, E. *Adv. Drug Delivery Rev.* **2008**, *60*, 473–484.
3. (a) Gruttadauria, M.; Giacalone, F.; Noto, R. *Chem. Soc. Rev.* **2008**, *37*, 1666; (b) Almasi, D.; Alonso, D.; Nájera, C. *Tetrahedron: Asymmetry* **2007**, *18*, 299–365; (c) Guillena, G.; Nájera, C.; Ramón, D. J. *Tetrahedron: Asymmetry* **2007**, *18*, 2249; (d) Pellissier, H. *Tetrahedron* **2007**, *63*, 9267; (e) Guillena, G.; Ramón, D. J. *Tetrahedron: Asymmetry* **2006**, *17*, 1465; (f) *Asymmetric Organocatalysis: from Biomimetic Concepts to Applications in Asymmetric Synthesis*; Berkessel, A., Gröger, H., Eds.; Wiley-VCH: Weinheim, 2005; (g) Dalko, P. I.; Moisan, L. *Angew. Chem., Int. Ed.* **2004**, *43*, 5138; (h) Special organocatalysis issue: . *Chem. Rev.* **2007**, *107*, 5413–5883; (i) Special organocatalysis issue: *Tetrahedron* **2006**, *62*, 243–502. *Enantioselective Organocatalysis: Reactions and Experimental Procedures*, ed. Dalko, P. I. Wiley-VCH, Weinheim, 2007.

4. (a) Burton, G.; Ku, T. W.; Carr, T. J.; Kiesow, T.; Sarisky, R. T.; Lin-Goerke, J.; Baker, A.; Earnshaw, D. L.; Hofmann, G. A.; Keenan, R. M.; Dhanak, D. *Bioorg. Med. Chem. Lett.* **2005**, *15*, 1553; b Dhanak, D.; Carr, T. J. Patent WO 2001085720, 2001; *Chem. Abstr.* **2001**, *135*, 371990.

5. (a) Parsons, A. F. *Tetrahedron* **1996**, *52*, 4149; (b) Baldwin, J. E.; Fryer, A. M.; Pritchard, G. J.; Spyvee, M. R.; Whitehead, R. C.; Wood, M. E. *Tetrahedron* **1998**, *54*, 7465.

6. Wardrop, D. J.; Burge, M. S. *Chem. Commun.* **2004**, 1230–1231.

7. Remuzon, P. *Tetrahedron* **1996**, *52*, 13803.

8. Nájera, C.; Sansano, J. M. *Chem. Rev.* **2007**, *107*, 4273–4303.

9. For recent reviews of 1,3-dipolar cycloaddition reactions of azomethine ylides, see: (a) Stanley, L. M.; Sibi, M. P. *Chem. Rev.* **2008**, *108*, 2887–2902; (b) Álvarez-Corral, M.; Muñoz-Dorado, M.; Rodríguez-García, I. *Chem. Rev.* **2008**, *108*, 3174–3198; (c) Naodovic, M.; Yamamoto, H. *Chem. Rev.* **2008**, *108*, 3132–3148; (d) Nair, V.; Suja, T. D. *Tetrahedron* **2007**, *63*, 12247–12275; (e) Pellisier, H. *Tetrahedron* **2007**, *63*, 3235–3285; (f) Pandey, G.; Banerjee, P.; Gadre, S. R. *Chem. Rev.* **2006**, *106*, 4484–4517; (g) Pinho e Melo, T. M. V. D. *Eur. J. Org. Chem.* **2006**, 2873–2888; (h) Bonin, M.; Chauveau, A.; Micouin, L. *Synlett* **2006**, 2349–2363; (i) Nájera, C.; Sansano, J. M. *Angew. Chem.* **2005**, *117*, 6428–6432; (j) Husinec, S.; Savic, V. *Tetrahedron: Asymmetry* **2005**, *16*, 2047–2061; (k) Coldham, I.; Hufton, R. *Chem. Rev.* **2005**, *105*, 2765–2809.

10. Najera, C.; Sansano J. M. in *Topics Heterocyclic Chem.* Ed. Hassner, A, **2008**, *12*, 117–145.

11. (a) Longmire, J. M.; Wang, B.; Zhang, X. *J. Am. Chem. Soc.* **2002**, *124*, 13400–13401; (b) Chen, C.; Li, X.; Schreiber, S. L. *J. Am. Chem. Soc.* **2003**, *125*, 10174–10175; (c) Knöpfel, T. F.; Aschwanden, P.; Ichikawa, T.; Watanabe, T.; Carreira, E. M. *Angew. Chem.* **2004**, *116*, 6097–6099; (d) Zheng, W.; Zhou, Y.-G. *Org. Lett.* **2005**, *7*, 5055–5058; (e) Stohler, R.; Wahl, F.; Pfaltz, A. *Synthesis* **2005**, 1431–1436; (f) Zheng, W.; Zhou, Y.-G. *Tetrahedron Lett.* **2007**, *48*, 4619–4622; (g) Zheng, W.; Chen, G.-Y.; Zhou, Y. G.; Li, Y.-X. *J. Am. Chem. Soc.* **2007**, *129*, 750–751; (h) Nájera, C.; Retamosa, M. G.; Sansano, J. M. *Org. Lett.* **2007**, *9*, 4025–4028; (i) Nájera, C.; Retamosa, M. G.; Sansano, J. M. *Angew. Chem., Int. Ed.* **2008**, *47*, 6055–6058.

12. (a) Oderaotoshi, Y.; Cheng, W.; Fujitomi, S.; Kasano, Y.; Minakata, S.; Komatsu, M. *Org. Lett.* **2003**, *5*, 5043–5046; (b) Cabrera, S.; Gómez-Arrayás, R.; Carretero, J. C. *J. Am. Chem. Soc.* **2005**, *127*, 16394–16395; (c) Gao, W.; Zhang, X.; Raghunath, M. *Org. Lett.* **2005**, *7*, 4241–4244; (d) Yan, X.-X.; Peng, Q.; Zhang, Y.; Zhang, K.; Hong, W.; Hou, X.-L.; Wu, Y.-D. *Angew. Chem. Int. Ed.* **2006**, *45*, 1979–1983; (e) Cabrera, S.; Gómez-Arrayás, R.; Martín-Matute, B.; Cossío, F. P.; Carretero, J. C. *Tetrahedron* **2007**, *63*, 6587–6602; (f) Llamas, T.; Gómez-Arrayás, R.; Carretero, J. C. *Org. Lett.* **2006**, *8*, 1795–1798; (g) Martín-Matute, B.; Pereira, S. I.; Peña-Cabrera, E.; Adrio, J.; Silva, A. M. S.; Carretero, J. C. *Adv. Synth. Catal.* **2007**, *349*, 1714–1724; (h) Shi, J.-W.; Shi, J. W. *Tetrahedron: Asymmetry* **2007**, *18*, 645–650; (i) Llamas, T.; Gómez-Arrayás, R.; Carretero, J. C. *Synthesis* **2007**, 950–957.

13. (a) Gothelf, A. S.; Gothelf, K. V.; Hazell, R. G.; Jørgensen, K. A. *Angew. Chem. Int. Ed.* **2002**, *41*, 4236–4238; (b) Panzner, M. J. *Org. Lett.* **2006**, *8*, 4687–4690.

14. Shi, J.-W.; Zhao, M.-X.; Lei, Z.-Y.; Shi, M. *J. Org. Chem.* **2008**, *73*, 305–308.

15. Saito, S.; Tsubogo, T.; Kobayashi, S. *J. Am. Chem. Soc.* **2007**, *129*, 5364–5365.

16. The employment of organocatalysts as well as chiral bases has been reported: (a) Alemparte, C.; Blay, G.; Jørgensen, K. A. *Org. Lett.* **2005**, *7*, 4569–4572; (b) Arai, S.; Takahashi, F.; Tsuji, R.; Nishida, A. *Heterocycles* **2006**, *67*, 495–501; (c) Ibrahem, I.; Ríos, R.; Vesely, J.; Córdova, A. *Tetrahedron Lett.* **2007**, *48*, 6252–6257; (d) Vicario, J. L.; Reboredo, S.; Badía, D.; Carrillo, L. *Angew. Chem. Int. Ed.* **2007**, *46*, 5168–5170; (e) Xue, M.-X.; Zhang, X.-M.; Gong, L.-Z. *Synlett* **2008**, 691–694.

17. For reviews of binap chemistry, see: Noyori, R. *Adv. Synth. Catal.* **2003**, *345*, 15–78.

18. Jeulin, S.; DupratdePaule, S.; Ratovelomanana-Vidal, V.; Gênet, J.-P.; Champion, N.; Dellis, P. *Proc. Natl. Acad. Sci.* **2004**, *101*, 5799–5804.

19. Dogan, O.; Koyuncu, H.; Garner, P.; Bulut, A.; Youngs, W. J.; Panzner, M. *Org. Lett.* **2006**, *8*, 4687.

20. Momiyama, N.; Yamamoto, H. *J. Am. Chem. Soc.* **2004**, *126*, 5360–5361.

21. (a) Burton, G.; Ku, T. W.; Carr, T. J.; Kiesow, T.; Sarisky, R. T.; Lin-Goerke, J.; Baker, A.; Earnshaw, D. L.; Hofmann, G. A.; Keenan, R. M.; Dhanak, D. *Bioorg. Med. Chem. Lett.* **2005**, *15*, 1553; b Dhanak, D.; Carr, T. J. Patent WO 2001085720, 2001; *Chem. Abstr.* **2001**, *135*, 371990.; For the first asymmetric synthesis of these inhibitors of the RNA-polymerase of the hepatitis C virus, using a diastereoselective 1,3-DC involving chiral lactate derived acrylates, see: (c) Nájera, C.; Retamosa, M. G.; Sansano, J. M.; de Cózar, A.; Cossío, F. P. *Eur. J. Org. Chem.* **2007**, *30*, 5038–5049.

22. Zoutendam, P. M. G. H.; Kissinger, P. T. *J. Org. Chem.* **1979**, *44*, 758.

23. Parr, R. G.; Yang, W. *Density-Functional Theory of Atoms and Molecules*; Oxford: New York, NY, 1989.

24. (a) Kohn, W.; Becke, A. D.; Parr, R. G. *J. Phys. Chem.* **1996**, *100*, 12974; (b) Becke, A. D. *J. Chem. Soc.* **1993**, *98*, 5648; (c) Becke, A. D. *Phys. Rev. A* **1988**, *38*, 3098.

25. Hay, P. J.; Wadt, W. R. *J. Chem. Phys.* **1985**, *82*, 299.

26. Hehre, W. J.; Radom, L.; Schleyer, P. v. R.; Pople, J. A. *Ab initio Molecular Orbital Theory*; Wiley: New York, NY, 1986, and references therein.

27. Frisch, M. J.; Trucks, G. W.; Schlegel, H. B.; Scuseria, G. E.; Robb, M. A.; Cheeseman, J. R.; Montgomery, J. A., Jr.; Vreven, T.; Kudin, K. N.; Burant, J. C.; Millam, J. M.; Iyengar, S. S.; Tomasi, J.; Barone, V.; Mennucci, B.; Cossi, M.; Scalmani, G.; Rega, N.; Petersson, G. A.; Nakatsuji, H.; Hada, M.; Ehara, M.; Toyota, K.; Fukuda, R.; Hasegawa, J.; Ishida, M.; Nakajima, T.; Honda, Y.; Kitao, O.; Nakai, H.; Klene, M.; Li, X.; Knox, J. E.; Hratchian, H. P.; Cross, J. B.; Bakken, V.; Adamo, C.; Jaramillo, J.; Gomperts, R.; Stratmann, R. E.; Yazyev, O.; Austin, A. J.; Cammi, R.; Pomelli, C.; Ochterski, J. W.; Ayala, P. Y.; Morokuma, K.; Voth, G. A.; Salvador, P.; Dannenberg, J. J.; Zakrzewski, V. G.; Dapprich, S.; Daniels, A. D.; Strain, M. C.; Farkas, O.; Malick, D. K.; Rabuck, A. D.; Raghavachari, K.; Foresman, J. B.; Ortiz, J. V.; Cui, Q.; Baboul, A. G.; Clifford, S.; Cioslowski, J.; Stefanov, B. B.; Liu, G.; Liashenko, A.; Piskorz, P.; Komaromi, I.; Martin, R. L.; Fox, D. J.; Keith, T.; Al-Laham, M. A.; Peng, C. Y.; Nanayakkara, A.; Challacombe, M.; Gill, P. M. W.; Johnson, B.; Chen, W.; Wong, M. W.; Gonzalez, C.; Pople, J. A. ɢᴀᴜssɪᴀɴ 03*, Revision C.02*; Gaussian: Wallingford, CT, 2004.

28. Maestro, version 8.5, Schrödinger, LLC, New York, NY, 2008.

29. Tsuge, O.; Kanemasa, S.; Yoshioka, M. *J. Org. Chem.* **1988**, *53*, 1384–1391.